INTERNATIONAL JOURNAL FOR NUMERICAL METHODS IN FLUIDS
Int. J. Numer. Meth. Fluids 2004; **44**:765–775 (DOI: 10.1002/fld.675)

Operator-splitting method for the analysis of cavitation in liquid-lubricated herringbone grooved journal bearings

Wu Jiankang[1], Li Anfeng[1], T. S. Lee[2,*,†,‡], C. Shu[2] and Wan Junmei[2]

[1] *Mechanics Department of Huazhong University of Science & Technology Wuhan 430074, China*
[2] *Mechanical Engineering Department, National University of Singapore, Singapore 119260, Singapore*

SUMMARY

This paper presents an operator-splitting method (OSM) for the solution of the universal Reynolds equation. Jakobsson–Floberg–Olsson (JFO) pressure conditions are used to study cavitation in liquid-lubricated journal bearings. The shear flow component of the oil film is first solved by a modified upwind finite difference method. The solution of the pressure gradient flow component is computed by the Galerkin finite element method. Present OSM solutions for slider bearings are in good agreement with available analytical and experimental results. OSM is then applied to herringbone grooved journal bearings. The film pressure, cavitation areas, load capacity and attitude angle are obtained with JFO pressure conditions. The calculated load capacities are in agreement with available experimental data. However, a detailed comparison of the present results with those predicted using Reynolds pressure conditions shows some differences. The numerical results showed that the load capacity and the critical mass of the journal (linear stability indicator) are higher and the attitude angle is lower than those predicted by Reynolds pressure conditions for cases of high eccentricities. Copyright © 2004 John Wiley & Sons, Ltd.

KEY WORDS: universal Reynolds equation; herringbone grooved journal bearing; operator-splitting method

INTRODUCTION

The effects of cavitation are important to the performance of liquid-lubricated herringbone grooved journal bearings (HGJBs). The Reynolds pressure condition assumes that the normal pressure derivative vanishes at cavitation boundaries. For a submerged journal bearing the

*Correspondence to: TS Lee, Department of Mechanical Engineering, National University of Singapore, 10 Kent Ridge Crescent, Singapore 119260.
†E-mail: mpeleets@nus.edu.sg
‡BE(Hons.I), PhD(UNSW), MASME, MIEAust, CPEng, MRINA, CEng, SrMAIAA, MEESS, MIES, MSAE, Associate Professor and Deputy Head, Fluid Mechanics Division.

Contract/grant sponsor: Ministry of Science-Technology of China; contract/grant no: PD9521901

Received March 2001
Revised 20 September 2003

pressure condition is well posed on the film rupture boundaries, but it is not valid on the film reformation boundaries. With the consideration for mass conservation, Jakobsson and Floberg [1] and Olsson [2] proposed a pressure boundary condition of cavitation to be applied to the Reynolds equation. This set of pressure conditions accounts for mass conservation over the whole of the film region. It has been called the Jakobsson–Floberg–Olsson JFO theory.

Elrod and Adams [3], Elrod [4] proposed a cavitation prediction algorithm incorporating JFO pressure conditions and introduced a universal equation that is applicable in both the full film and cavitated flow region. The universal Reynolds equation is able to automatically predict cavitation region, avoiding the difficulties of locating film rupture and reformation boundaries. It has been termed Elrod's cavition algorithm. The universal Reynolds equation was solved by Vijayaraghavan and Keith [5, 6] using a finite difference method, in which the shear flow is determined by central differencing in the full film zone and upwind differencing in the cavitation zone. Yu and Keith [7] developed a boundary element method to predict gaseous cavitation based on the universal Reynolds equation.

The flow in the oil film of a journal bearing consist of a shear flow and a pressure gradient flow. Shear flows and pressure gradient flows represent two kinds of flow phenomenon. The shear flow is governed by a first-order hyperbolic differential operator with a uniform speed. The pressure gradient flow is governed by a second-order parabolic differential operator. The shear flows and pressure gradient flows can be solved separately within a time step. In this way each type of flow can be treated by the most effective numerical method. The operator-splitting method has been used to solve the advection–diffusion equations successfully [8–10]. It is expected that this is also applicable to the universal Reynolds equation when applied to the HGJB problems.

Recent investigations showed that HGJB greatly improves the film stability of the journal bearing for cases of low eccentricities when compared to the plain journal bearing. The film pressure of the herringbone grooved journal bearings is a saw-like distribution. The cavitation zones are extremely complicated and discontinuously distributed. The dynamic characteristics of herringbone grooved journal bearing have been studied by some researches [11–13]. These works are based on Reynolds equation of an incompressible fluid. Recently, Jang and Chang [14] studied HGJB based on the universal Reynolds equation using a finite-volume method. Their calculated load capacity is slightly larger than Hirs's experimental data [15] in high eccentricities. The differences in the results obtained in applying the Reynolds condition and the JFO condition in predicting the dynamic characteristics of a liquid-lubricated HGJB are investigated in the present study through a proposed operator splitting method.

OPERATOR-SPLITTING METHOD FOR SOLVING THE UNIVERSAL REYNOLDS EQUATION

The two-dimensional, unsteady Reynolds equation for a compressible Newtonian lubricant in laminar flow can be written as

$$\frac{\partial \rho h}{\partial t} + \frac{\partial}{\partial x}\left(\frac{\rho h u}{2}\right) = \nabla\cdot\left(\frac{\rho h^3}{12\mu}\nabla p\right) \tag{1}$$

Elrod's algorithm treats lubricant as compressible fluid with a high bulk modulus. The density is related to the film pressure through the following definition:

$$g\beta = \rho \frac{\partial p}{\partial \rho} \tag{2}$$

where β is bulk modulus of the lubricant and g is a switch function defined as

$$g = \begin{cases} 1 & (\theta \geqslant 1.0) \text{ in the full film zone,} \\ 0 & (\theta < 1.0) \text{ in the cavitation zone} \end{cases} \tag{3}$$

θ is a density ratio defined by

$$\theta = \frac{\rho}{\rho_c} \tag{4}$$

where ρ_c is lubricant density in the cavitation zone (constant) at the cavitation pressure p_c. The pressure can be expressed as

$$p = p_c + g\beta \ln \theta \tag{5}$$

Substituting Equations (4), (5) in to Equation (1), the universal Reynolds equation is obtained.

$$\frac{\partial \theta h}{\partial t} + \frac{\partial}{\partial x}\left(\frac{\theta h u}{2}\right) = \nabla \cdot \left(\frac{g h^3 \beta}{12\mu} \nabla \theta\right) \tag{6}$$

Equation (6) represents mass conservation over the whole film including full film zone and cavitation zone. Only the switch function g is updated to correct the flows in cavitation zones during the actual computation. The dimensionless form of universal Reynolds equation (6) can be expressed as

$$\frac{\partial \theta \bar{h}}{\partial \bar{t}} + \frac{\partial}{\partial \bar{x}}(\theta \bar{h}) = \nabla \cdot (\bar{H} \bar{\nabla} \theta) \tag{7}$$

$$\text{where } \bar{H} = g\bar{\beta}\bar{h}^3/12\pi \tag{8}$$

For simplicity, the bar notation '-' will be dropped in Equation (7) in the following analysis. For the proposed operator-splitting method (OSM), the dimensionless universal Reynolds equation (7) is divided into two components: the shear flow equation and the pressure gradient flow equation.

$$\frac{\partial}{\partial t}(\theta h) + \frac{\partial}{\partial x}(\theta h) = 0 \tag{9}$$

$$\frac{\partial}{\partial t}(\theta h) = \nabla \cdot (H \nabla \theta) \tag{10}$$

The shear flow equation (9) is a one-dimensional advection equation with a constant speed boundary condition imposed along the circumference. In the OSM, it is first solved using a

modified upwind finite difference method

$$(\theta h)_i^{n+1} = (\theta h)_i^n - C_r[(\theta h)_i^n - (\theta h)_{i-1}^n] - \frac{C_r(1-C_r)}{2}[(\theta h)_{i+1}^n - 2(\theta h)_i^n + (\theta h)_{i-1}^n] \tag{11}$$

where $C_r = u\Delta t/\Delta x$, (here $u = 1$); the superscripts n, $n+1$ denote the time levels. The last term in the right-hand side of Equation (11) eliminates the numerical diffusion problems resulting from the first-order upwind scheme. The solution of Equation (11) serve as the initial condition for the solution of the pressure gradient flow equation (10). The pressure gradient equation (10) is next solved using the Galerkin finite element method. For numerical continuity of the Equation (10) on the cavitation boundaries, Vijayaraghavan and Keith [5] rewrote the Equation (10) as

$$h\frac{\partial \theta}{\partial t} = \nabla\cdot[H_0\nabla(g(\theta - 1)] \tag{12}$$

where $H_0 = \bar{\beta}\bar{h}^3/12\pi$. For cases of a rotating plain member and a non-moving grooved member, the film thickness is independent of time. Applying the Galerkin finite element method to Equation (12) yields

$$\left\langle h\frac{\partial \theta}{\partial t}, \phi_i \right\rangle = \langle \nabla\cdot[H_0\nabla(g(\theta - 1)], \phi_i\rangle \tag{13}$$

The notation $\langle\ \rangle$ denotes the integral over the entire two-dimensional domain. ϕ_i $(i = 1, 2, 3, \ldots, N)$ are global interpolation functions, N is total number of nodes. The time derivative is approximated by finite difference, i.e.

$$\frac{\partial \theta}{\partial t} = \frac{\theta^{n+1} - \theta^n}{\Delta t} \tag{14}$$

Substituting Equation (14) into Equation (13) and integrating it in part, yields

$$\langle h\theta^{n+1}, \phi_i\rangle = \langle h\theta^n, \phi_i\rangle + \Delta t \oint_{\partial\Omega} H_0 \frac{\partial g^n(\theta^n - 1)}{\partial n}\phi_i \, \mathrm{d}s - \Delta t\langle H_0\nabla[g^n(\theta^n - 1)], \nabla\phi_i\rangle \tag{15}$$

The boundary integral terms vanish at the internal nodes. Equations (15) are replaced by the essential boundary conditions on the side boundaries where the pressure is specified as ambient pressure. The matrix form of Equation (15) can be written as

$$[A]\{\theta^{n+1}\} = [B]\{g^n(\theta^n - 1)\} \tag{16}$$

where the matrix coefficients are given as

$$A_{ij} = \langle h\phi_j, \phi_i\rangle \tag{17}$$

$$B_{ij} = A_{ij} - \Delta t\langle H_0\nabla\phi_j, \nabla\phi_i\rangle \tag{18}$$

Table I. Parabolic slider bearing.

Parameters	Values	Units
Length L	7.62×10^{-2}	m
Min. film thickness	2.54×10^{-5}	m
Max. film thickness	5.04×10^{-5}	m
Viscosity μ	0.039	Pa s
Bulk modulus β	6.9×10^{7}	N/m^2
Cavitation pressure	0	N/m^2
Inlet θ	1.0	
Outlet θ	0.55	

The mass lumping technique has been successfully applied to matrixes involving no space derivatives in many practical problems. By adding all elements of every row of matrix $[A]$ to the diagonal elements, the matrix $[A]$ is reduced to a vector. The matrix solver is not needed. Furthermore, the shear flow and pressure gradient flow terms are solved using the same grids. Steady-state solutions are obtained by searching for converged solutions of the unsteady governing equations.

NUMERICAL VALIDATIONS

The validity of the present OSM numerical method for solving journal bearings problems are shown through the following illustrative numerical solutions for a parabolic slider bearing given by Elrod [4] and Vijayaraghavan [5]. The parameters used for the parabolic slider bearing are presented in Table I.

Figures 1 and 2 show that the present numerical results obtained agree very well with those of Elrod's [4].

APPLICATION OF OSM TO HERRINGBONE GROOVED JOURNAL BEARINGS

Figure 3 shows a typical geometry of a HGJB. α is the groove angle; w_r, w_g are the ridge width and groove width, respectively; c is the average radial clearance; h_g is groove depth. The rotating member is plain and the stationary member has a number of herringbone grooves. The film thickness is independent of time, so film flows and pressure are steady. The steady-state solutions are obtained through solving of the unsteady universal Reynolds equation.

In order to make a valid comparison with available experimental data, the experimental parameters of a HGJB given by Hirs [14] are adopted in the numerical examples: $L/D = 1.0$, groove number $N_g = 8$, groove angle $\alpha = 68.19°$, groove depth $h_g/c = 1.0$, $W_g/W_r = 1.0$, Bulk modulus $\bar{\beta} = 20\,000$. Two grooved bearings are used in the experiment. The cavitation pressure is set at a predetermined value (the ambient gauge pressure is assumed zero). Only half of the lubrication domain is needed due to symmetry. A parallelogram grids of 128 (in circumference) $\times$ 20 (in axis) is used. The grid lines are made to coincide with grooves the as shown in Figure 4.

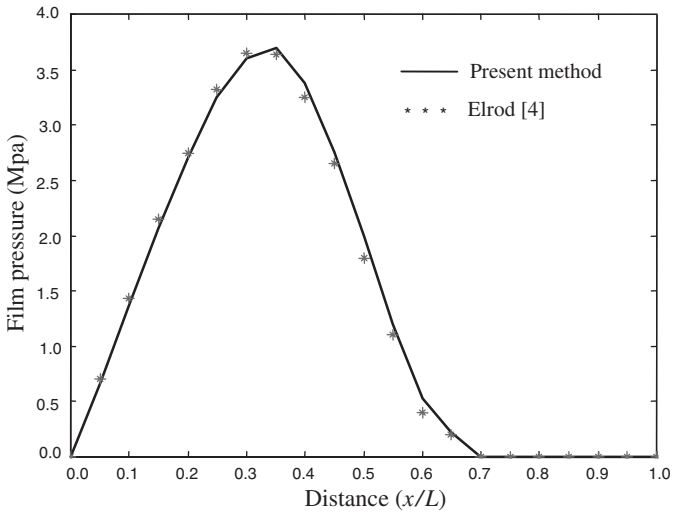

Figure 1. Pressure distribution in a parabolic slider bearing.

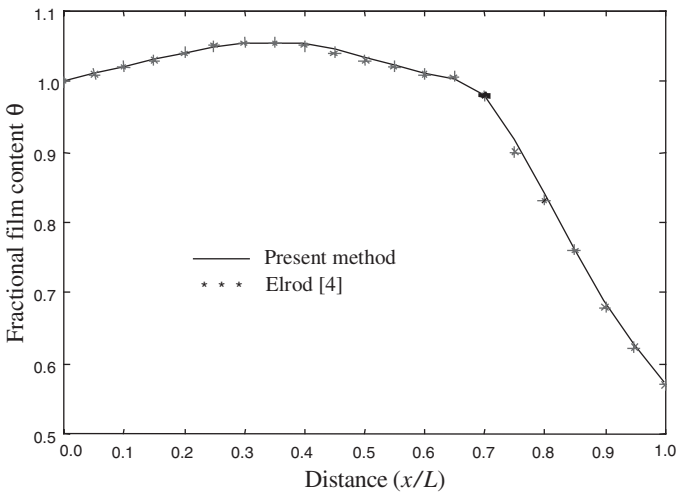

Figure 2. Distribution of fractional film content θ in a parabolic slider bearing.

The dimensionless film thickness is modelled as

$$h = 1.0 + h_g + \varepsilon \cos \varphi \tag{19}$$

where the groove depth h_g is zero in the groove ridge, φ is circumference angle. The film pressure and cavitation areas are shown in Figures 5 and 6 for $\varepsilon = 0.6$.

It can be seen that the film pressure solutions predicted by two different types of cavitation pressure condition are very similar, but the peak values of pressure predicted by JFO condition are slightly higher than those predicted by Reynolds condition, and the cavitation areas

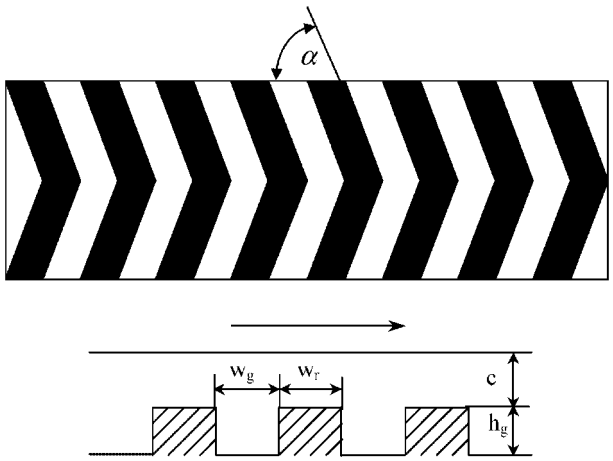

Figure 3. Sketch of a HGJB.

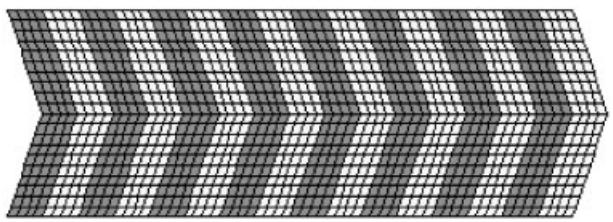

Figure 4. Sketch of the finite element grids of lubrication domain.

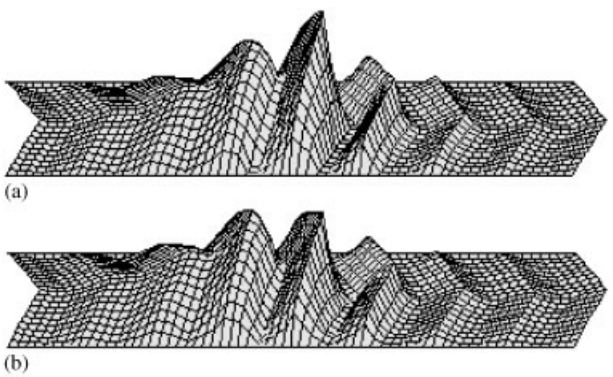

Figure 5. (a) The film pressure of a HGJB predicted by JFO condition $\varepsilon = 0.6$; (b) The film pressure of a HGJB predicted by Reynolds condition $\varepsilon = 0.6$.

predicted with the JFO condition are larger than those of Reynolds condition for the cases of high eccentricities. The calculated load capacities and attitude angles are shown in Figures 7 and 8.

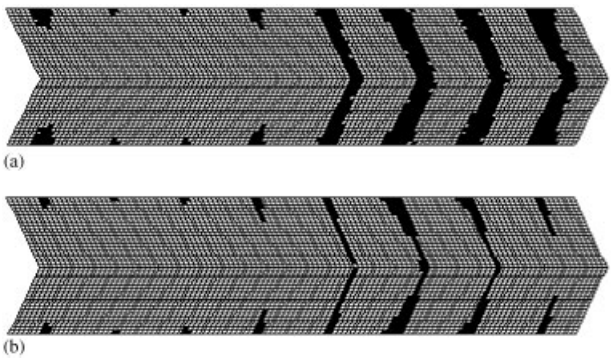

Figure 6. (a) The cavitation areas (black) of a HGJB predicted by JFO pressure condition $\varepsilon = 0.6$; (b) The cavitation areas (black) of a HGJB predicted by Reynolds pressure condition $\varepsilon = 0.6$.

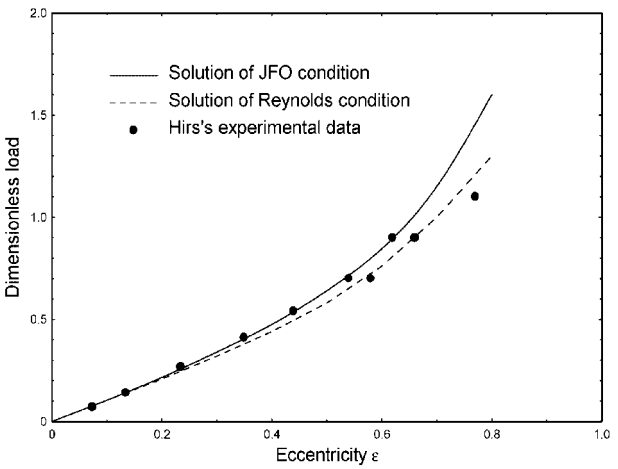

Figure 7. The load capacity of a liquid-lubricated HGJB.

It can be seen that the load capacities predicted by the JFO condition are in general agreed with the experimental data given by Hirs [14]. The predicted load predicted with JFO condition is slightly larger than experimental data for cases of high eccentricities.

It is found that the load capacities predicted by JFO condition are higher, the attitude angles are smaller than those predicted by Reynolds condition when eccentricities are greater than 0.4.

Once the film pressure is solved, the linear stability analysis of the journal bearing operations can then be carried out. The dynamic coefficients are obtained by solving the first-order pressure perturbation equations and integrating the perturbation pressure over the journal surface. The critical mass of the journal can then be calculated based on the dynamic coefficients. The critical mass of the journal is shown in Figure 9.

It is also found that the critical mass of journal predicted by the JFO condition is larger than that predicted by Reynolds condition when the eccentricities are greater than 0.4.

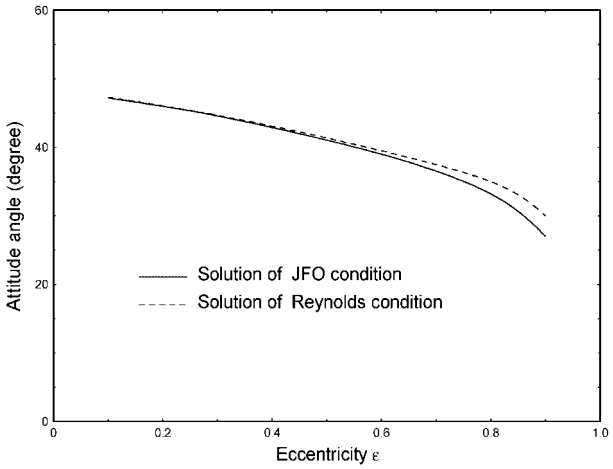

Figure 8. The attitude angle of a liquid-lubricated HGJB.

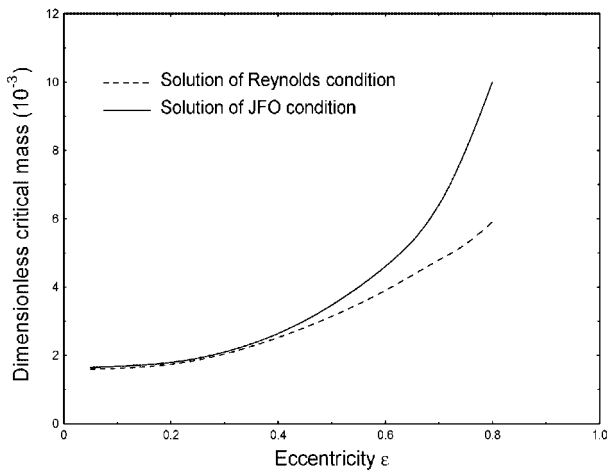

Figure 9. The critical mass of a liquid-lubricated HGJB.

For cases of low eccentricities ($\varepsilon \leqslant 0.4$), no significant cavitation is found. It is expected that the numerical solutions predicted by JFO condition are not essentially different from those predicted by Reynolds condition. Indeed the numerical solutions with the two types of boundary conditions are almost the same for low eccentricities.

In the cases of high eccentricities the shear flows of cavitation zones play an important role in determining the characteristics of the lubrication film flows. A non-zero pressure gradient on film reform boundaries (JFO condition) affects the flows of full film zones in a different way from the Reynolds condition. For a HGJB, the cavitations are significant, and the numerical solutions predicted by JFO and Reynolds conditions show difference only for the cases of high eccentricities.

CONCLUSIONS

The present investigations show that the proposed operator-splitting method (OSM) is capable to effectively solve the universal Reynolds equation for oil film dynamics in liquid-lubricated journal bearings. With the proposed OSM, the shear flow of the oil film in the journal bearing is first solved by a stable modified upwind method over the entire lubrication domain. The pressure gradient flow can than be next solved by the Galerkin finite element method without convective instability problems. Universal Reynolds equation incorporating the JFO cavitation pressure conditions into the OSM solution processes was found to be suitable for the analysis of the dynamic characteristics of a liquid-lubricated HGJB. For the cases of high eccentricities, the predicted load capacities and critical mass of journal by the proposed OSM were observed to be greater while the attitude angles are smaller than those predicted by the Reynolds pressure condition. The differences in solutions with JFO and Reynolds conditions by OSM method are negligible for low eccentricity cases.

ACKNOWLEDGEMENTS

This work is a part of research project supported by national ministry of Science-Technology of China, Grant No. PD9521901. This work was completed during Professor Wu's attachment to the Department of Mechanical and Production Engineering of the National University of Singapore (NUS). The authors are grateful to NUS for providing the financial and computer facility support for Professor Wu during the course of this work.

NOMENCLATURE

c	radial clearance
h	film thickness
$\bar{h}$	dimensionless film thickness, (h/c)
L/D	length to diameter ratio
p	film pressure
$\bar{p}$	dimensionless film pressure, $(p/\omega\mu)(c/R)^2$
$\bar{M}_c$	dimensionless critical mass of journal, $M_c/[64\pi^2\mu R^4 c^{-3}\omega^{-1}]$
p_a	ambient pressure
y	co-ordinate in axial direction
$\bar{y}$	dimensionless of y $(y/2\pi R)$
w_r	dimensionless groove ridge width
β	bulk modulus
μ	lubricant viscosity
ρ	fluid density
t	time
$\bar{t}$	dimensionless time $(\omega t/4\pi)$
e	eccentricity
ε	eccentricity ratio (e/c)
g	switch function
R	bearing radium

x co-ordinate in circumference
$\bar{x}$ dimensionless of x $(x/2\pi R)$
$\bar{W}$ dimensionless load capacity, $(W/\omega\mu LD)(c/R)^2$
p_c cavitation pressure
α groove angle
h_g dimensionless groove depth
w_g dimensionless groove width
$\bar{\beta}$ dimensionless bilk modulus $(\beta/\omega\mu)(c/R)^2$
ω angular rotation speed
u journal surface velocity

REFERENCES

1. Jakobsson B, Floberg L. The finite journal bearing considering vaporization. *Transaction of Chalmers University of Technology* 1957; 190–198.
2. Olsson KO. Cavitation in dynamically loaded bearings. *Transaction of Chalmers University of Technology* 1965; 308–320.
3. Elord HG, Adams ML. A computer program for cavitation and starvation problems. *Cavitation and Related Phenomena in Lubrication*. Mechanical Engineering Publications. New York, 1974; 37–41.
4. Elord HG. Cavitation algorithm. *Journal of Lubrication Technology* (*ASME*) 1981; **103**(3):350–354.
5. Vijayaraghavan D, Keith TG. Development and evaluation of a cavitation algorithm. *Tribology Transactions* 1989; **32**(2):225–233.
6. Vijayaraghavan D, Keith TG. Grid transformation and adaption techniques applied in the analysis of cavitation journal bearing. *Journal of Tribology* (*ASME*) 1990; **112**:52–58.
7. Qiulin Yu, Keith TG. Prediction of cavitation in journal bearing using a boundary element method. *Journal of Tribology* (*ASME*) 1995; **117**:411–421.
8. Wu Jiankang. Wave equation model for solving advection–diffusion equation. *International Journal for Numerical Methods in Engineering* 1994; **37**(16):2717–2733.
9. Wu Jiankang. A wave equation model to solve multidimensional transport equation. *International Journal for Numerical Methods in Fluids* 1997; **24**:1–17.
10. Lee TS. A false transient model for the study of steady fluid motion and heat transfer in trapezoidal chambers with heated bases. *International Journal of Computational Fluid Dynamics* 1996; **7**:339–347.
11. Bonneau D, Absi J. Analysis of aerodynamic journal bearings with small number of herringbone grooves by finite element method. *Journal of Tribology* (*ASME*) 1994; **116**:698–704.
12. Kang K, Rhim Y, Sung K. A study of oil-lubricated herringbone grooved journal bearing, part one: numerical analysis. *Journal of Tribology* (*ASME*) 1996; **118**:906–911.
13. Nicole Z, Luis SA. Finite element analysis of herringbone grooved journal bearings: a parametric study. *Journal of Tribology* (*ASME*) 1998; **120**:234–240.
14. Jang GH, Chang DI. Analysis of hydrodynamic herringbone grooved journal bearing considering cavitation. *STLE/ASME Tribology Conference* 1999, Paper No. 99-TRIB-37.
15. Hirs GG. The load capacity and stability characteristics of hydrodynamic grooved journal bearing. *ASLE Transactions* 1965; **8**:296–305.

